forests

MDPI

Article

Carbon in Woody Debris and Charcoal Layer in Cold Temperate Coniferous Forest 13 Years After a Severe Wildfire

Yuanchun Peng, Lina Shi, Xingyu Hou and Yun Zhang *

Key Laboratory of Sustainable Forest Ecosystem Management—Ministry of Education, College of Ecology, Northeast Forestry University, 26 Hexing Road, Harbin 150040, China; pyc2022@nefu.edu.cn (Y.P.); shi120017@nefu.edu.cn (L.S.); hxy2000@nefu.edu.cn (X.H.)

* Correspondence: rowena@nefu.edu.cn; Tel.: +86-13384657565

Abstract: Pyrogenic carbon (PyC) is generated from the incomplete combustion of biomass and fossil fuels. Pyrogenic carbon is highly stable and is often referred to as a missing carbon sink. It plays a crucial role in global carbon cycling and climate change research. We analyzed the storage of PyC and uncharred biological organic carbon (BOC) within woody debris (WD) and the charcoal layer, as well as the properties of PyC, across four forest types in the cold temperate coniferous forest of the Greater Khingan Mountains. Pyrogenic carbon in WD appears as charred, blackened material, while PyC in the charcoal layer was extracted through chemical oxidation using HF/HCl treatment. Our methodology included particle size separation through dry sieving, followed by the analysis of four size fractions (>2 mm, 2–1 mm, 1–0.5 mm and <0.5 mm) for elemental composition, and the chemical composition was analyzed using DRIFT. With respect to WD, PyC storage ranged from 0.040 to 0.179 Mg·ha^{-1}, whereas BOC storage ranged from 3.1 to 16.8 Mg·ha^{-1}. In the charcoal layer, PyC storage ranged from 7.9 to 44.3 Mg·ha^{-1}, and BOC storage ranged from 3.8 to 11.6 Mg·ha^{-1}. Pyrogenic carbon storage in the charcoal layer dominated (>99%) on the above-ground in each forest type. The DRIFT analysis confirmed that the coarse fraction (>2 mm) contain more polymeric aromatic structures, and most likely indicated the presence of benzene carboxylic compounds (1710 cm^{-1}), which may originate from the charred plant material. Our research aims to enhance the understanding of the retention effects of recalcitrant carbon in WD and charcoal layer of cold temperate coniferous forest, thereby providing new insights into the impact of fire disturbances on carbon cycling within forest ecosystems.

Keywords: pyrogenic carbon; biological organic carbon; charcoal layer; carbon storage; chemical property

Academic Editor: Tina Louise Bell

Received: 5 March 2025
Revised: 13 April 2025
Accepted: 14 April 2025
Published: 15 April 2025

Citation: Peng, Y.; Shi, L.; Hou, X.; Zhang, Y. Carbon in Woody Debris and Charcoal Layer in Cold Temperate Coniferous Forest 13 Years After a Severe Wildfire. *Forests* **2025**, *16*, 685. https://doi.org/10.3390/f16040685

1. Introduction

On average, about 464 million hectares (approximately 4%) of the Earth's vegetated land surface are consumed by wildfires each year [1]. Due to the balance between carbon emissions from wildfires and the carbon absorbed by regenerating vegetation, it was once considered a "net-zero carbon emission event". However, this supposed balance does not account for pyrogenic carbon (PyC). Wildfires can lead to a gaseous carbon loss of 58.4 t C·ha and can form 50–200 Tg of PyC [2]. Wildfires profoundly altered the terrestrial carbon cycle on approximately 40% of the Earth's surface [3].

Pyrogenic carbon refers to a broad category of carbon-rich remnants that are formed from the continuous products generated by the combustion of biomass and fossil fuels [4,5], including soot, char, black carbon, and biochar. Pyrolysis causes cellulose, hemicellulose

and lignin to lose unstable derivatives (e.g., O-alkyl C) and form stable structures, such as condensed aryl and O-arylfuran. The residence time that PyC remains in the environment typically exceeds that of its unburnt precursors by one or two orders of magnitude [1]. Consequently, PyC generated from wildfires has the potential to act as a long-term carbon sequestration mechanism, lasting for decades to millennia [6,7]. A meta-analysis of data from 24 stable carbon isotopes and 128 radioactive carbon isotopes concluded that approximately 97% of the mean residence times (MRTs) for PyC can exceed 556 years, as reported by Wang et al. [8]. Pyrogenic carbon can be categorized into three distinct pools [9]. The first pool of a minor proportion of labile carbon, typically accounting for less than 5% of the total PyC, with a decomposition half-life ranging from weeks to months [10]. The second pool comprises semi-labile PyC [11], exhibiting an intermediate decomposition rate with a half-life of several years to decades. The third pool represents highly stable PyC, characterized by strong resistance to mineralization and a half-life extending from centuries to millennia, potentially reaching geological timescales [9].

Charring affects materials to a certain depth below their surface, resulting in a blackened rind on the surface of biomass or fossil fuels. In various forest tree species, including *Pseudotsuga menziesii*, *Pinus ponderosa*, and high-Cascade mixed conifers, the char depths showed a relatively narrow range (from 1 to 17 mm, with a mean of 8.2 mm) two to four years after the wildfire, as reported by Donato et al. [12]. This was observed despite the presence of diverse substrates, including sound wood, rotten material, bark, resulting from varying fire intensities, from low surface fires to active crown fires. Importantly, char depth did not correspond with particle diameter, likely due to comparable oxygen conditions impacting combustion at specific depths. The active ingredients in PyC decompose rapidly, potentially resulting in a short-term stimulating effect on the decomposition of organic matter [13]. Consequently, semiactive and inert components gradually become predominant due to their encapsulation, sorptive protection, and toxic effects [14]. These factors prevent microorganisms and extracellular enzymes from accessing organic matter, thereby diminishing microbial activity [8,15]. This process isolates the internal biomass (the uncharred portion) from microorganisms and the surrounding environment, effectively sequestering active carbon for long periods of time. To date, surface carbonization treatment remains a significant method for wood preservation in forest regions [16].

Physical processes, such as weathering, leaching, mechanical fragmentation, disturbances by soil animals, and abiotic degradation, lead to the gradual abscission of PyC from the surfaces of burned materials [9,17]. These abscised PyCs are subsequently deposited on or near the soil surface, forming a unique charcoal layer in the burned region [18,19]. If there is a surface or underground wildfire, then it is crucial to consider the direct products of pyrolytic carbonization from the litter layer or peat layer. As vegetation recovers in the burned region, the new litter layer covers the charcoal layer. This litter layer reduces surface erosion of the charcoal layer, allowing this unique charcoal layer to be preserved for a longer period [20]. Pyrogenic carbon in the charcoal layer continues to exert effects such as encapsulation, adsorption protection, and toxicity, blocking (or weakening) the connection between above-ground biomass and soil microorganisms [8,14,15]. Pyrogenic carbon forms a new isolation between the above-ground biomass and the soil layer, once again playing a vital role in the sequestration of above-ground BOC.

Currently, research on PyC in mineral soils has been extensively conducted, representing 81.7% of global studies on carbon cycling in fire-affected forest [21,22]. However, studies on PyC in the charcoal layer, which includes both the litter and the organic layers, exhibit a systematic lag. A comprehensive meta-analysis published in 2023, which incorporated 196 global observational datasets, indicates that the data coverage for PyC in both the litter layer and organic layer is less than 18.3% (n = 36) [23]. In particular, research on

the residual PyC from charred woody debris during the mid-term recovery phase after wildfire is nearly non-existent. This study focuses on cold temperate coniferous forest in the Greater Khingan Mountains, 13 years after a wildfire (in the absence of further disturbance by wildfire), representing the pioneer species recovery succession stage. We propose the following hypotheses for the specific scenario 13 years after a wildfire:

1. The PyC formed a distinct charcoal layer on the ground, which has been the primary component of the above-ground PyC storage.
2. Uncharred BOC has been effectively sequestered and demonstrated a strong correlation with PyC storage.
3. The activated carbon in PyC has largely decomposed, and PyC that now exists is stable carbon.

2. Materials and Methods

2.1. Site Description

The study was conducted at Huyuan Forest Farm, which is part of the Huzhong Forestry Bureau situated in the Greater Khingan Mountains of China (51°17′57″–51°50′09″ N, 123°10′05″–123°48′14″ E) (Figure 1). This area experiences a cold temperate continental monsoon climate, marked by prolonged, frigid winters with an ice duration lasting approximately 6 months, reaching minimum temperatures of −52°. Forest wildfires occur frequently in spring and autumn because Mongolian drought winds cause high temperatures and strong winds. The longest wildfire cycle in the study area range from 110 to 120 years. The soil type is classified as Umbri-Gelic Cambosols in Chinese Soil Taxonomy, which corresponds to Leptic Cambic Umbrisols (Brunic) according to the World Reference Base for Soil Resources (WRB) [24]. The flora of the area is representative of cold temperate coniferous forest, predominantly featuring *Larix gmelinii* and *Pinus pumila* [25]. Thirteen years after the wildfire, the vegetation has notably recuperated, now encompassing *Populus davidiana* along with sparse populations of *Betula platyphylla*, while various shrubs like *Rhododendron dauricum* and *Ledum palustre* dominate the understorey.

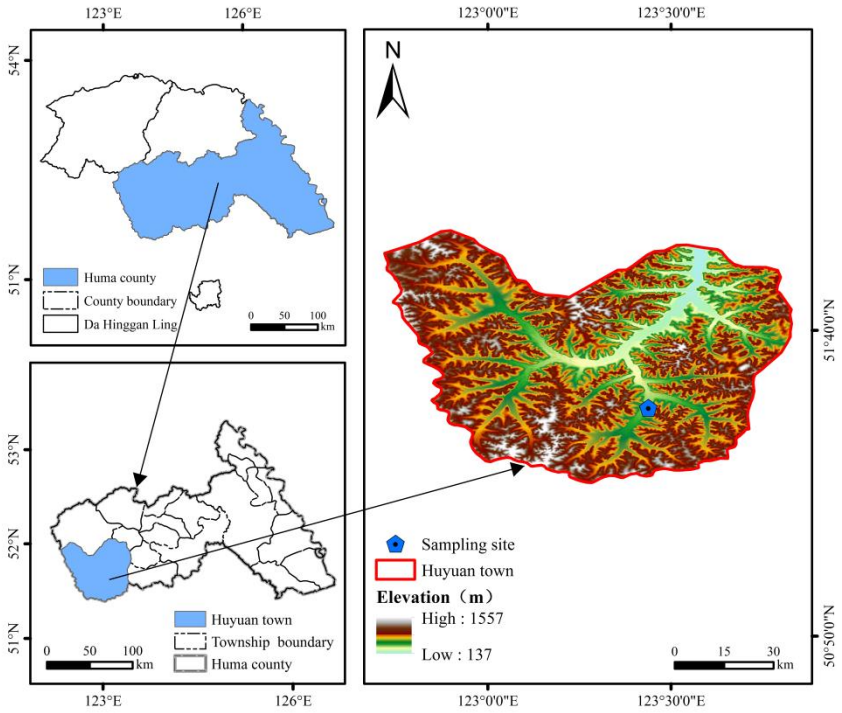

Figure 1. Location map of the study site.

In June 2010, a catastrophic wildfire ignited by a lightning strike swept through the Huyuan Forest Farm, burning approximately 480 hectares of coniferous forest. The fire spread rapidly due to dry and windy conditions, causing extensive damage to the forest ecosystem. Post-fire tree mortality reached nearly 100%, leaving only scarred trunks and debris. According to historical forestry records, the sampling site had not experienced any forest fires in the preceding 50 years. In September 2023, we established three replicated transects within the study area extending from the valley to the upper slope positions, based on microtopographic features and the spatial distribution of pre-fire vegetation types. Each transect includes four distinct forest types: *Pinus pumila-Larix gmelinii* (PL), *Rhododendron dauricum-Larix gmelinii* (RL), *Ledum palustre-Larix gmelinii* (LL), and *Grass-Larix gmelinii* (GL). A total of 12 standard plots of 20 × 30 m were set up. The conditions of these plots are presented in Table 1.

Table 1. Selected characteristics of the study sites.

Forest Type	Latitude and Longitude	Slope Position	Altitude (m)	Slope (°)	Mortality (%)	Pre-Fire Community Structure	Post-Fire Community Structure	Update Biomass (Mg·ha^{-1})	Thickness of PyC Layer (cm)
PL	123°15′43″–123°26′17″ E 51°27′17″–51°45′64″ N	Upper slope	1030.6–1061.3	10–22	100	Tree *Larix gmelinii*, *Betula platyphylla* Shrub *Pinus pumila*, *Vaccinium uliginosum* Herb *Cyperaceae*, *Roseceae*	Tree *Populus davidiana* Dode, *Betula platyphylla* Shrub *Vaccinium uliginosum* Herb *Cyperaceae*, *Roseceae*	35.6	4.3
RL	123°25′20″–123°25′27″ E 51°27′20″–51°27′25″ N	Middle slope	948.6–960.4	13–17	100	Tree *Larix gmelinii*, *Betula platyphylla* Shrub *Pinus pumila*, *Rhododendron dauricum* Herb *Cyperaceae*, *Roseceae*	Tree *Populus davidiana* Dode, *Betula platyphylla* Shrub *Rhododendron dauricum* Herb *Cyperaceae*, *Roseceae*	33.5	6.1
LL	123°15′30″–123°15′38″ E 51°27′31″–51°27′34″ N	Lower slope	853.2–871.3	18–19	100	Tree *Larix gmelinii*, *Betula platyphylla* Shrub *Pinus pumila*, *Ledum palustre* Herb *Cyperaceae*, *Roseceae*	Tree *Populus davidiana* Dode, *Betula platyphylla* Shrub *Ledum palustre*, *Vaccinium uliginosum* Herb *Cyperaceae*, *Roseceae*	27.4	7.1
GL	123°15′35″–123°15′43″ E 51°27′40″–51°27′45″ N	Valley	727.2–731.5	14–16	100	Tree *Larix gmelinii*, *Betula platyphylla* Shrub *Vaccinium uliginosum*, *Ledum palustre* Herb *Cyperaceae*, *Deyeuxia angustifolia*	Tree *Populus davidiana* Dode, *Betula platyphylla* Shrub *Vaccinium uliginosum*, *Ledum palustre* Herb *Roseceae*, *Deyeuxia angustifolia*	6.8	1.8

Note: Forest type classified on vegetation community structure present before the fire [26].

2.2. Experimental Design and Sampling

2.2.1. Sampling of Woody Debris

Woody debris is classified on the basis of the status and size within the community and are primarily divided into four compositions: snag, stump, down wood, and twig.

- Standing trees. All snags (>1.37 m in height) and stumps (<1.37 m in height) were measured in each sample plot [27]. The following parameters were recorded for each tree: species, height, diameter at breast height (DBH), basal diameter, char height, char upper diameter, and char depth, the investigation methods followed the approach described by Donato et al. [12]. Specifically, the distance between charred and uncharred wood was measured to the nearest millimeter. These measurements were used to calculate the biomass of standing trees. In each sample plot, for different tree species, disks approximately 5 cm thick were collected at 1/4, 2/4, and 3/4 of the trunk height (representing the lower, middle, and upper sections, respectively) to determine the content of BOC. Bark samples were randomly collected from 20 cm wide strips at 1/2 char height to determine the content of PyC. Each sample was replicated three times.

- Down wood. Three 5 × 5 m sample squares were established within each sample plot to measure the length, large head diameter, small head diameter, middle diameter, and char depth of all down wood. A classification system using five classes was used to assess decay level [28], which was used to calculate the biomass of down wood. Samples were randomly collected from each tree species at different decay levels in charred and uncharred forms within each sample square, with each sample being repeated three times to determine down wood carbon content.
- Twig. Sample squares of 1 × 1 m were established within each 5 × 5 m sample square. All twigs within these sample squares were collected to determine their biomass and carbon content.

2.2.2. Sampling of the Charcoal Layer

In the 1 × 1 m sample squares mentioned above, the twigs and leaves on the ground were removed prior to sampling. The color of the charcoal layer is distinctly different from that of the litter layer and the mineral soil layer, appearing darker than the typical organic layer. A significant quantity of charcoal particles is observable within the charcoal layer. We recorded both the upper and lower boundaries of the charcoal layer and calculated its thickness. Additionally, three samples were taken with a ring knife (100 cm^3) to determine the bulk density. If the thickness of the charcoal layer exceeds 5 cm, sampling from the surface will ensure that the mineral soil layer is not collected. Conversely, if the thickness of the charcoal layer is less than 5 cm, the ring knife should be driven to a point 0.5 cm above the soil layer, and the height not filled by the charcoal layer within the ring knife should be recorded to calculate the density of the charcoal layer.

2.3. Laboratory Analysis and Determination

All samples were returned to the laboratory, they were dried at 65 °C until a constant weight was achieved, and the results were recorded.

- Charred WD. Pyrogenic carbon from the bark samples of standing trees was manually selected and weighed to determine the PyC mass per unit volume [29–31]. Pyrogenic carbon was visually characterized as black particles with a silvery gloss [32]. The PyC samples were carefully scraped from down wood and twigs using a blade [3], then ground with a mortar and passed through a 0.25 mm sieve. Carbonate content was assessed by adding 10% HCl to representative PyC subsamples. The absence of effervescence suggested a negligible carbonate content (<1%) [33]. Consequently, inorganic carbon was considered insignificant in the samples, and total carbon was equivalent to organic carbon.
- Uncharred WD. Samples were ground using an ultra-fine grinder and passed through a 0.25 mm sieve.
- Charcoal layer. All charcoal was gently sieved and separated into four particle size fractions: >2 mm, 2–1 mm, 1–0.5 mm and <0.5 mm. The dry weights of each fraction were recorded. The samples for each particle size fraction were ground using a mortar and passed through a 0.15 mm sieve. Pyrogenic carbon samples were extracted using the chemical oxidation method using HF/HCl treatment and a mixed solution of $K_2Cr_2O_7$ and H_2SO_4 [34,35].

The carbon content was determined through combustion use a multi-N/C 3000 analyser (Analytik Jena AG, Jena, Germany). The dried samples were pressed into pellets for nitrogen and hydrogen content analysis using a laser high-spectral element analyser (J200 Tandam LA-LIBS Instrument, Applied Spectra, West Sacramento, CA, USA). The ash content was determined gravimetrically after dry combustion in a muffle furnace at 800 °C for 4 h. The oxygen content was calculated by difference. The DRIFT spectra of all

fractions were acquired using a Bruker TENSOR series FT-IR spectrophotometer (Ettlingen, Baden-Württemberg, Germany), coupled with a diffuse reflectance accessory (Spectra-Tech, Inc., Stamford, CT, USA).

The measurement of down wood density (ρ) begins with determining the volume of the samples using the water displacement method, averaging the results from three measurements. Subsequently, all samples are placed in an oven at 65 °C and dried to a constant weight. The density of down wood is calculated as the ratio of the dry weight of the samples to their volume [36].

2.4. Carbon Storage Calculation

2.4.1. Woody Debris Carbon Storage Calculation

- Standing trees. The biomass of the uncharred snag was determined using the allometric growth equation [37]. The regression relationship between the volume and biomass of the snag was employed to calculate the biomass of the uncharred stump. The surface area of the charred WD was calculated based on field measurement data [12], and multiplied by the *mass of PyC per unit volume* to obtain the PyC_{mass} of standing trees (Equation (1)).

$$PyC_{mass} = \pi \times (r_1 + r_2) \times \sqrt{(r_1 - r_2)^2 + h^2} \times depth_{char} \times mass\ of\ PyC\ per\ unit\ volume \quad (1)$$

where r_1 is the basal diameter (cm); r_2 is the char upper diameter (cm); and h is the char height (m).

- Down wood. The calculation of the down wood volume was conducted for the entire particle cylinder, which included the charred part (Equation (2)). For an inner uncharred cylinder whose diameter depends on char depth (Equation (3)). The volume difference between these two measurements represented the PyC volume (Equation (4)) [12,38].

$$Vol_{tot} = \pi L\left({D_S}^2 + {D_L}^2\right)/80,000 \quad (2)$$

$$Vol_{core} = \pi L\left([D_S - (2 \times depth_{char} \times 0.7)]^2 + [D_L - (2 \times depth_{char} \times 0.7)]^2\right)/80,000 \quad (3)$$

$$Vol_{PyC} = Vol_{tot} - Vol_{core} \quad (4)$$

where Vol_{tot} is the total volume (m^3); Vol_{core} is the volume of the core (m^3); Vol_{PyC} is the volume of PyC (m^3); D_S is the diameter of the small end (cm); D_L is the diameter of the large end (cm); and L is the length of the down wood (m).

To obtain PyC_{mass}, Vol_{PyC} is multiplied by the wood density (ρ_{wood}), the proportion of mass remaining (0.3) and the ratio (r) of the PyC surface area of down wood (Equation (5)).

$$PyC_{mass} = Vol_{PyC} \times \rho_{wood} \times 0.3 \times r \quad (5)$$

- Twig. By calculating the mass ratio of PyC to unburned twig [3], we determined the biomass of PyC and unburned twig in each sample plot.

The uncharred WD and PyC carbon storage ($Mg \cdot ha^{-1}$) for each component can be calculated by multiplying the biomass per unit area of snag, stump, down wood and twig by their respective carbon content.

2.4.2. Charcoal Layer Carbon Storage Calculation

The calculation formula of carbon layer is as below (Equation (6)).

$$TOC = TOC_c \times BD \times T \times (1 - G) \times 10^{-2} \quad (6)$$

where *TOC* is the total organic carbon storage (kg·m^{-2}); TOC_C is the organic carbon content; BD is the bulk density (g·cm^{-3}); T is the charcoal layer depth (cm); and G is the gravel content >2 mm (%).

2.5. Data Analysis

In this study, the main independent variable was forest types. Given that, after a fire disturbance, above-ground carbon is primarily present in the fire-induced dead WD and the charcoal layer, BOC and PyC are categorized as the dependent variables (response variables) Y. We used Excel for data calculation.

One-way ANOVA was used to analyse whether there was a significant effect of different forest types on BOC and PyC storage. Two-way ANOVA was used to analyse the effects of forest type and the form of WD present on bioorganic and PyC carbon storage, and Bonferroni's method was used to analyse the variability between different datasets. The significance level was set at $\alpha = 0.05$, and all the statistical analyses were performed using SPSS 26 statistical software and plotted using Origin 2022 [39].

3. Results

3.1. Carbon in Woody Debris

3.1.1. Pyrogenic Carbon on Woody Debris

At the time point of 13 years after wildfire, PyC on WD was distributed within a fairly narrow range. The char height of the standing trees ranged from 56.4 to 80.4 cm, while the char depth was distributed between 0.8 and 1.2 mm. Among the different forest types, the RL had the greatest char height and char depth, as well as the greatest PyC storage (147.4 ± 4.3 mg/cm^3). Overall, the char depth of down wood was greater than that of standing trees, ranging from 1.0 to 1.9 mm, with the deepest char depth (1.9 ± 0.7 mm) measured in PL (Table 2).

Thirteen years after the wildfire, PyC storage in WD ranged from 0.040 to 0.179 Mg·ha^{-1} in cold temperate coniferous forest. Among the different forest types, RL presented the greatest PyC storage, which was approximately 1.5–4 times greater than that of LL and GL ($p < 0.05$). Pyrogenic carbon storage for snag and stump was greatest for RL, reaching 0.036 Mg·ha^{-1} and 0.007 Mg·ha^{-1}, respectively. In contrast, PyC storage in down wood and twig was greatest in PL, with values of 0.043 Mg·ha^{-1} and 0.114 Mg·ha^{-1}, respectively (Figure 2).

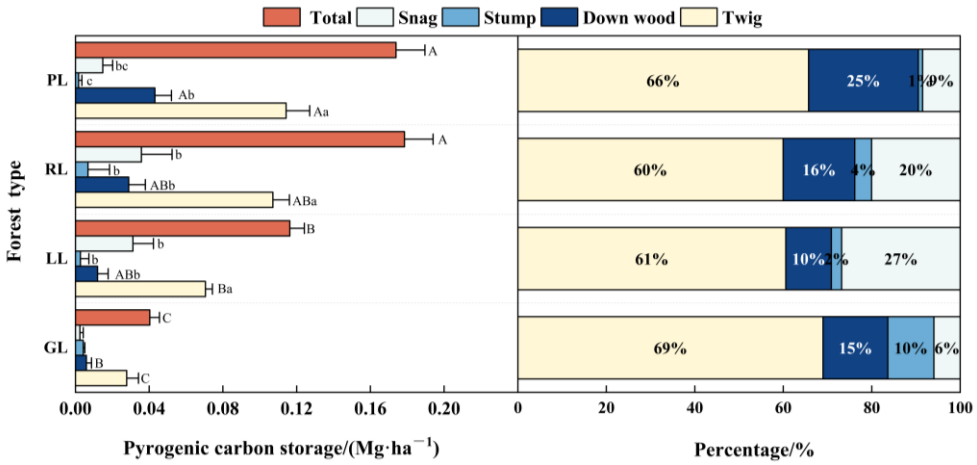

Figure 2. Pyrogenic carbon storage in woody debris. Capital letters indicate significant differences among the composition of woody debris ($p < 0.05$), while lowercase letters indicate significant differences among forest type ($p < 0.05$).

Table 2. Distribution characteristics of woody debris.

Forest Type	Standing Trees Density ($N \cdot hm^{-2}$)	Charred WD					Uncharred WD			
		Standing Trees			Down Wood		Standing Trees		Down Wood	
		Tree Species Composition	Char Height (cm)	Char Depth (mm)	PyC Density (mg/cm^3)	Tree Species Composition	Char Depth (mm)	Height (m)	DBH (cm)	Length (m)	Middle Diameter (cm)
PL	461.1	98 Larix gmelinii 2 Betula platyphylla	65.1 ± 10.3	1.1 ± 0.06	139.6 ± 4.9	82 *Pinus pumila* 10 *Larix gmelinii* 8 *Betula platyphylla*	1.9 ± 0.7	7.1 ± 1.5	10.3 ± 0.3	2.1 ± 0.3	6.1 ± 1.3
RL	344.4	91 Larix gmelinii 9 Betula platyphylla	80.4 ± 19.3	1.2 ± 0.06	147.4 ± 4.3	65 *Pinus pumila* 26 *Larix gmelinii* 9 *Betula platyphylla*	1.4 ± 0.3	9.8 ± 3.3	18.5 ± 6.4	2.0 ± 0.3	5.6 ± 0.9
LL	661.1	95 Larix gmelinii 5 Betula platyphylla	69.6 ± 21.3	1.0 ± 0.01	135.9 ± 10.0	65 *Pinus pumila* 29 *Larix gmelinii* 7 *Betula platyphylla*	1.0 ± 0.2	10.2 ± 0.9	11.2 ± 1.6	2.3 ± 1.0	5.2 ± 1.1
GL	527.8	85 Larix gmelinii 15 Betula platyphylla	56.4 ± 1.9	0.8 ± 0.07	129.4 ± 5.3	95 *Larix gmelinii* 5 *Betula platyphylla*	1.3 ± 0.5	1.5 ± 0.3	5.4 ± 0.4	2.0 ± 0.3	3.0 ± 0.3

Note: The data given in the table are means ± standard deviation (with 95% confidence intervals), and the numbers in the species composition indicate the proportion of the biomass density of that species.

The PyC composition of each forest type was similar. Twig had the greatest proportion of PyC, ranging from 60 to 69%. In addition, down wood accounted for 10 to 25%, whereas snag constituted between 6 and 27%. Stump represented the smallest proportion, although the slightly higher percentage of stump in GL was associated with local forest clearing activities.

3.1.2. Biological Organic Carbon Protected by Pyrogenic Carbon

Thirteen years after the wildfire, in terms of the uncharred WD, the height of WD in both standing trees and down wood was greatest in LL. The DBH of standing trees was greatest in RL, and the middle diameter of down wood was greatest in PL (Table 2).

Thirteen years after the wildfire, BOC storage of WD ranged from 3.1 to 16.8 Mg·ha^{-1} in cold temperate coniferous forest. Notably, BOC storage was significantly greater in PL than in GL ($p < 0.05$), with the former exhibiting approximately five times greater BOC storage than the latter. Different forest types had varying effects on BOC storage of WD in the same form. Among these forms, BOC storage of snag was greatest in RL at 6.3 Mg·ha^{-1}, which was significantly greater than that in LL and GL ($p < 0.05$). Additionally, BOC storage of down wood was greatest in PL at 12.1 Mg·ha^{-1}, significantly exceeding that of the other three forest types ($p < 0.05$). No significant difference was measured in BOC storage between stump and twig, with greatest values recorded in RL at 0.3 Mg·ha^{-1} and 2.2 Mg·ha^{-1}, respectively. Furthermore, the same forest type had varying effects on BOC storage of different forms of WD, and BOC storage of down wood accounted for 41–72% (Figure 3).

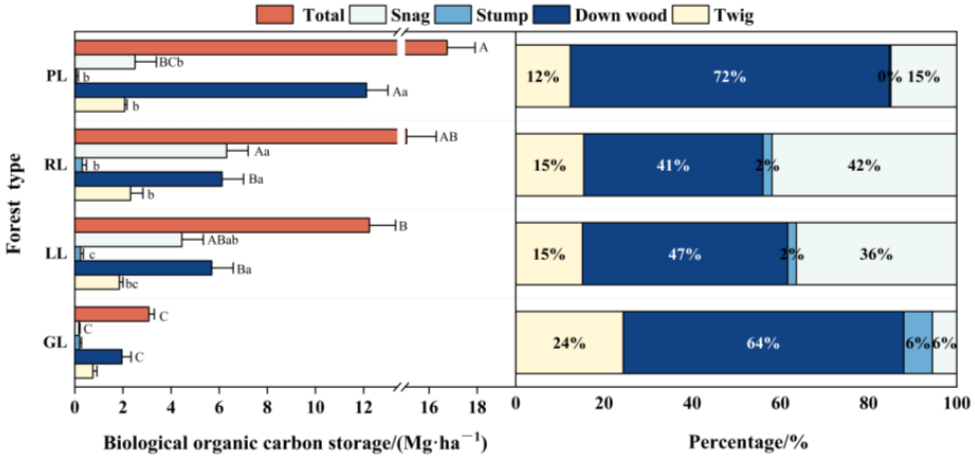

Figure 3. Biological organic carbon storage in woody debris. Capital letters indicate significant differences among the composition of woody debris ($p < 0.05$), while lowercase letters indicate significant differences among forest type ($p < 0.05$).

3.2. Carbon in the Charcoal Layer

The PyC storage of the charcoal layer in the study area ranged from 7.9 to 44.3 Mg·ha^{-1}. Pyrogenic carbon storage was greatest in RL, significantly exceeding that in both PL and GL ($p < 0.05$). Furthermore, BOC storage ranged from 3.8 to 11.6 Mg·ha^{-1}, the total organic carbon (TOC) storage showed consistent changes with the PyC storage. In terms of the composition of the organic carbon in the charcoal layer, PyC was dominant, accounting for 67 to 87% of the TOC. In the charcoal layer of RL, PyC accounted for approximately 87% of the organic carbon pool (Figure 4).

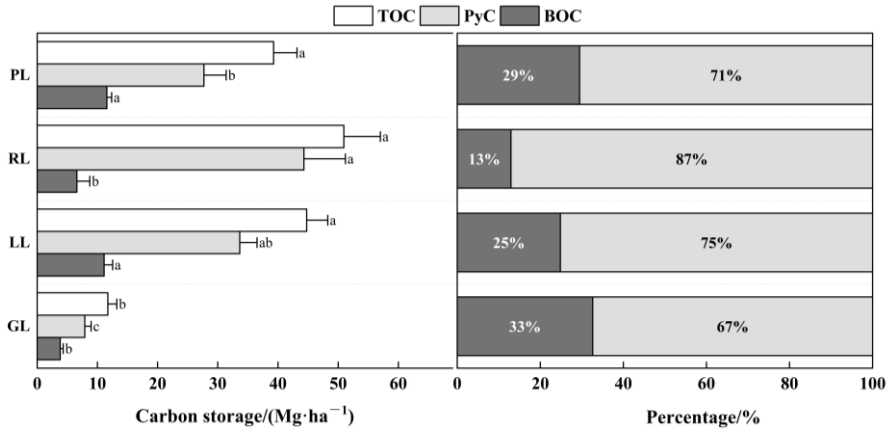

Figure 4. Carbon storage and distribution in charcoal layer. Lowercase letters indicate significant differences among forest type ($p < 0.05$).

3.3. Carbon Storage and Distribution Patterns in the Woody Debris and Charcoal Layer

Thirteen years after the wildfire, the above-ground PyC storage in all forest types was dominated by the charcoal layer, accounting for 99.2 to 99.6%, whereas less than 1% was attributed to WD. In contrast, the BOC storage above-ground was predominantly attributed to WD, although the proportion in GL was slightly lower, likely associated with localized forest clearing activities (Figure 5).

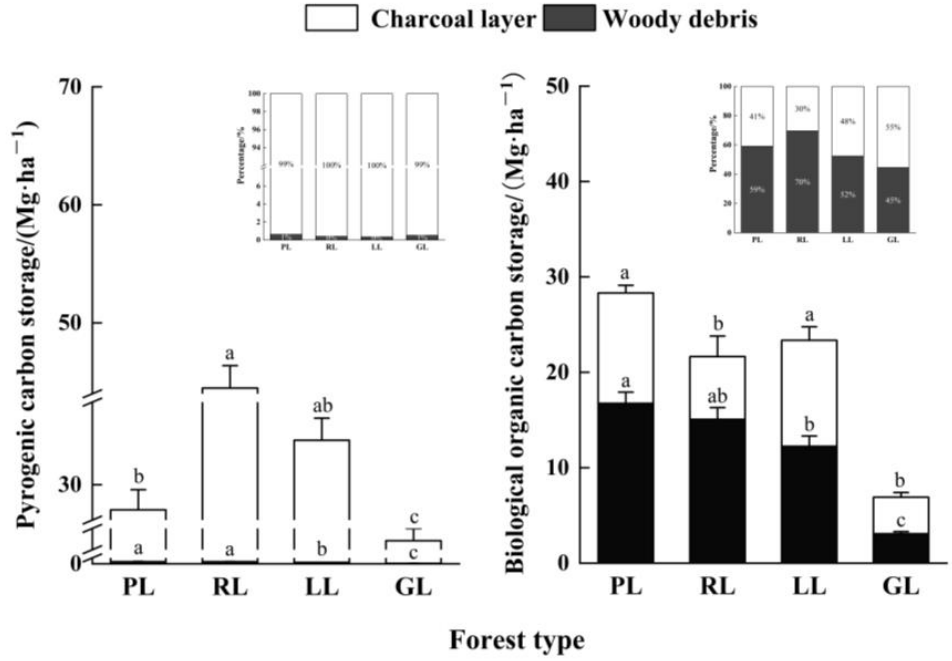

Figure 5. Carbon storage distribution of woody debris and charcoal layer. Lowercase letters indicate significant differences among forest types ($p < 0.05$).

A linear positive correlation was found between above-ground BOC storage and PyC storage ($p < 0.05$). The goodness of fit (R^2) was determined to be 0.33 (Figure 6a). This correlation may be attributed to the strong associations among prefire vegetation types and biomass characteristics with PyC storage at this stage. Additionally, a linear positive correlation exists between WD biomass and charcoal layer PyC storage (Figure 6b).

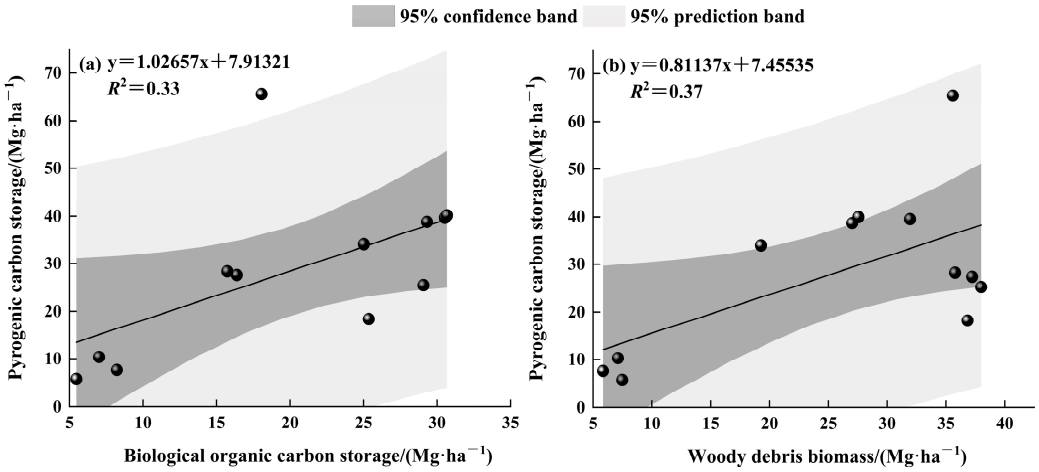

Figure 6. (**a**) Linearly fitted model for biological organic carbon storage compared to pyrogenic carbon storage, (**b**) linearly fitted model for woody debris biomass compared to pyrogenic carbon storage.

3.4. Pyrogenic Carbon Element Analysis

In terms of PyC distribution in the charcoal layer (Table 3), PyC fractions < 0.5 mm accounted for the largest proportion (39.8%), whereas >2 mm fractions represented <9% of the total. Carbon content ranged from 219.68 to 449.30 g·kg^{-1}, and N content ranged from 4.27 to 6.11 g·kg^{-1} of the different fractions, with the >2 mm fraction exhibiting the greatest content of both C and N, which were significantly greater than those of the other fractions. Additionally, the atomic measurement ratio indicates that the greatest C/N ratio occurs for particles > 2 mm in size, which was significantly greater than that of the other three particle sizes. In contrast, the H/C and O/C ratios exhibited opposite trends.

Table 3. Elemental content and atomic ratio of pyrogenic carbon fractions.

Fraction	C Distribution % of Total	C (g·kg^{-1})	N (g·kg^{-1})	C/N	H/C	O/C
>2 mm	8.55 ± 10.26	449.30 ± 90.58 a	6.11 ± 1.70 a	76.84 ± 16.54 a	0.06 ± 0.01 c	0.23 ± 0.04 c
1–2 mm	26.40 ± 9.56	249.04 ± 104.00 b	4.27 ± 1.40 b	58.97 ± 15.86 b	0.12 ± 0.03 b	0.43 ± 0.12 b
0.5–1 mm	25.28 ± 8.39	229.71 ± 53.83 b	4.43 ± 1.17 b	54.64 ± 15.06 bc	0.13 ± 0.05 b	0.46 ± 0.12 b
<0.5 mm	39.77 ± 10.76	219.68 ± 90.60 b	4.81 ± 1.61 b	48.08 ± 15.93 c	0.16 ± 0.04 a	0.54 ± 0.17 a

Note: The data given in the table are mean ± standard deviation (confidence interval is 95%), n = 36. Lowercase letters indicate significant differences among particle sizes (p < 0.05).

The van Krevelen plot analysis, based on H/C versus O/C atomic ratios, classified the four fractions into three distinct clusters with characteristic chemical signatures. The >2 mm fraction showed low values that match those of black carbon (BC) with a high degree of condensation (Figure 7a). The (N + O)/C atomic ratios of the four fractions exhibit a positive relationship with the N/C atomic ratio (Figure 7b). Notably, the ratio of the >2 mm fraction is generally lower than those of the other three fractions, suggesting that N and O elements are synergistically pyrolyzed.

The DRIFT spectra are shown in Figure 8. The shoulder peak at 1710 cm^{-1} corresponds to the C=O stretching vibration in carboxyl groups attached to aromatic structures [40]. The prominent absorption bands near 1600 and 1480 cm^{-1} are associated with C=C or C=N stretching vibrations in polyaromatic systems [41,42], which are formed through thermal rearrangement and cyclization of organic matter. Pyridine exhibits absorption bands near 1600 cm^{-1} and 1500 cm^{-1}, potentially resulting from the thermal dehydration of aromatic amides or from the cleavage of rings accompanied by the rearrangement of heterocyclic nitrogen [43]. In the fingerprint area, a peak at 1015 cm^{-1} is indicative of the

stretching vibration absorption of the C−O−C group found in the structures of cellulose and hemicellulose. The range of 900–650 cm^{-1} typically corresponds to the absorption peak of C−H bonds in the aromatic ring. In this study, the peak at 830 cm^{-1} is associated with the out-of-plane bending vibration absorption of the C−H bonds in double-substituted aromatic rings, whereas the peak at 778 cm^{-1} corresponds to the out-of-plane bending vibration absorption of C−H bonds in mono-substituted aromatic rings.

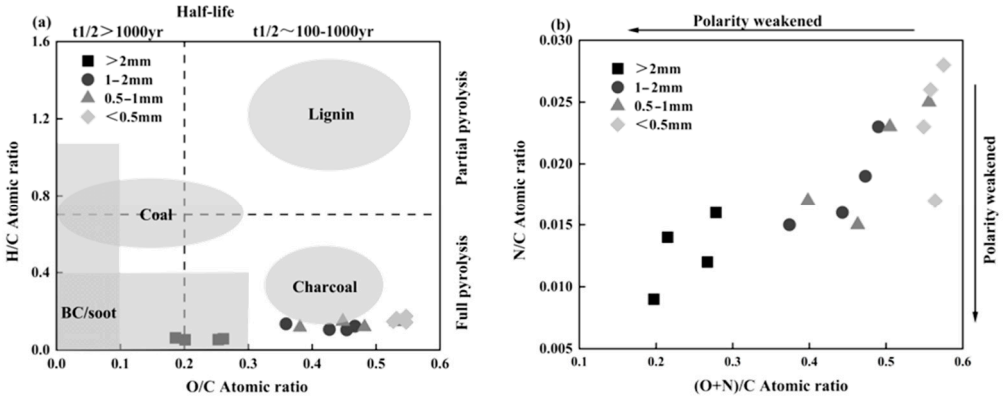

Figure 7. (**a**) Van Krevelen diagram of H/C and O/C of PyC fractions, (**b**) Van Krevelen diagram of N/C and the (O + N)/C of PyC fractions.

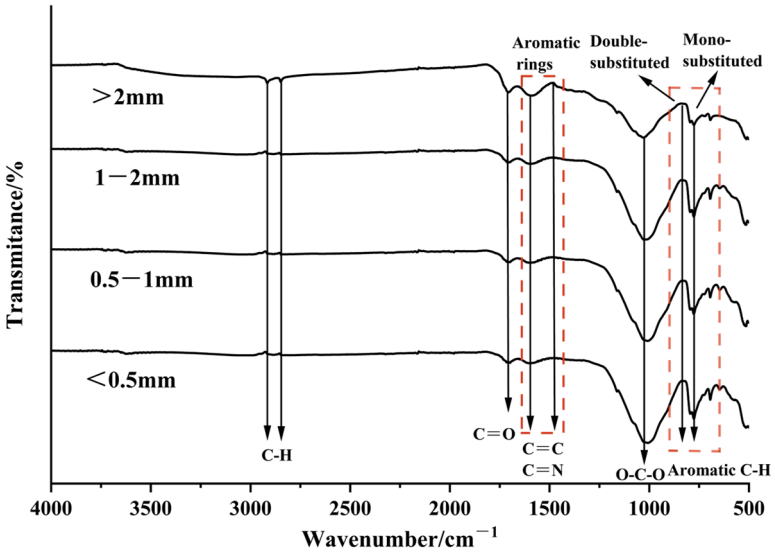

Figure 8. DRIFT spectra of the four pyrogenic carbon fraction.

4. Discussion

4.1. Carbon in Woody Debris

Thirteen years after the wildfire, the char depth of PyC on WD was distributed within a relatively limited range of 0.8–1.2 mm. The results of this study are lower than those reported by Donato et al. [12], who reported that for various forest tree species, including *Pseudotsuga menziesii*, *Pinus ponderosa*, and high-Cascade mixed conifers, char depths measured 2–4 years post-wildfire showed a relatively limited range of 1–17 mm, with an average depth of 8.2 mm. This implies that, over a decadal timescale, 90% or more of PyC detaches from the surface of WD.

Thirteen years after the wildfire in cold temperate coniferous forest, PyC storage on WD was 0.13 $Mg \cdot ha^{-1}$. There is a notable lack of research regarding the long-term retention effects of PyC in post-fire WD. Current studies primarily focus on the post-fire production of PyC. For example, in a conifer forest in western USA, coarse WD (>7.5 cm diameter)

can produce 6.4 Mg·ha^{-1} of PyC [44]. In the boreal forest of Canada, the PyC production from standing tree bark is estimated at 2.5 ± 1.3 Mg·ha^{-1}, while the PyC generated from down wood is estimated at 1.9 ± 0.2 Mg·ha^{-1} [1]. Pyrogenic carbon storage measured in this study decreased by 57 to 98% compared to these previous values. This finding further supports the spatial distribution of PyC storage in WD and surface charcoal layer. Among the four forest types, PyC storage in WD was greatest in PL, whereas PyC storage was lowest in GL. This is closely related to the biomass of WD both pre-fire and/or post-fire. According to the results of the WD biomass survey in this study, it is inferred that PL has the greatest biomass after fire. In contrast, GL experienced forest clearing in the second year after the fire, resulting in the lowest biomass. Additionally, the relatively high lipid content of *Pinus pumila* contributes to its relatively high PyC yield [40].

Biological organic carbon storage of WD was 11.78 Mg·ha^{-1} after 13 years of wildfire. Yang et al. [27] reported that the BOC storage capacity, including PyC, of the above-ground WD in the Huzhong forest area of the Greater Khingan Mountains was 12.90 Mg·ha^{-1}, recorded 3 to 5 years post-wildfire. Using this reference value, it can be inferred that 91% of BOC remains retained in the WD after 8–10 years since the previous investigation. When accounting for differences in PyC quantification methods in the survey, as well as the subsequent shedding and fragmentation of the WD surface, it is likely that the retention rate of the WD increased. We posit that, in addition to the very slow natural semi-decomposition rate of 50–70 years for *Larix gmelinii*, the unique isolation mechanism formed by PyC on the surface of WD and at the ground level should also be critically considered.

4.2. Carbon in the Charcoal Layer

Thirteen years after the wildfire, the typical cold temperate coniferous forest charcoal layer had accumulated 28.4 Mg·ha^{-1} of PyC, a process that is closely associated with the time scale following the fire. Caroline et al. [29] conducted a cross-millennial study of the boreal forest in western Quebec, Canada. In plots sampled 24 to 2355 years post-fire, the storage of >2 mm PyC at the organic-mineral interface fluctuated between 5 and 5.5 Mg·ha^{-1}. Although this simple comparison is rough, it still suggests that after more than a decade, over 80% of PyC in the charcoal layer may have been exported. This implies the presence of complex biogeochemical redistribution mechanisms that occur during the reorganization of ecosystem carbon pools following a fire.

The charcoal layer accounting for more than 99% of the above-ground PyC storage. This value differs by more than 50% from the 38–42% surface accumulation of PyC reported by Santín et al. and Righi et al. [1,45] shortly after the fire (within 1–6 days). Assuming that the burning intensities of the two forest fires are similar, this difference indicates that PyC has migrated to the surface from its previous distribution down wood, bark and needles. Our results revealed a unique charcoal layer with a thickness ranging from 1.8 to 7.1 cm (average of 4.8 cm) situated between the litter layer and the soil layer. This finding suggests that PyC has largely completed its transition from the WD pool to the charcoal layer pool. Notably, the loss of PyC from the charcoal layer is also important. On the one hand, PyC may be susceptible to surface erosion because of its limited interactions with soil minerals and low-density particles [31,46]. On the other hand, some smaller diameter particles in the charcoal layer may have entered the soil carbon pool through leaching [47,48].

As the altitude increased, the sample plots examined in this study included GL, LL, RL, and LL. Our results revealed the greatest PyC storage in the charcoal layer of the RL. This occurrence can be linked to the interplay between PyC biomass and the surface erosion that occurs after combustion. Although we were unable to accurately quantify PyC storage following the four forest type fires, our analysis of the existing WD biomass and the flammability of tree species suggests that PyC storage in PL may be the

greatest. However, we did not measure the greatest PyC storage in the charcoal layer of PL, which may be attributed to surface erosion influenced by the terrain. Owing to precipitation and gravity, the upper slope is more likely to input PyC to the lower slopes and valleys [31,49,50]. Furthermore, the thickness of the charcoal layer directly reflects the PyC storage characteristics of the charcoal layer, which are influenced by the combined effects of forest type and topography.

Notably, in this study "13 years after the wildfire" specifically refers to the 13-year period following the last forest fire. We hypothesize that the majority of PyC storage in the charcoal layer is derived from this fire event. However, we cannot discount the potential influence of historical fire disturbances, as the maximum fire return interval in this region ranges from 110 to 120 years. Current data suggest that this is the only forest fire that has occurred in the last 50 years. The legacy effects of historical fire disturbances represent a source of error that cannot be overlooked. In addition, human activity interference is also a non-negligible factor affecting carbon storage. Compared with other forest types, GL has undergone extensive forest clearing activities, resulting in very low storage of both biological carbon and black carbon in the surface charcoal layer, despite its terrain conditions being more favorable for the accumulation of these carbons [51].

4.3. Properties of Pyrogenic Carbon

Carbon content increases as the particle size increases, and its degree of aggregation also increases. This study demonstrates that the >2 mm fraction exhibits a higher abundance of polymeric aromatic structures compared to other fractions. These findings align with previous observations on coarse and fine charcoal fractions manually separated from tropical soils subjected to slash-and-burn agricultural practices. Nocentini et al.'s [30] SEM observations revealed that the charred portions originated from various plant tissues, with coarse fractions derived primarily from wood and bark residues, whereas finer fractions were composed predominantly of needles and leaves. This finding is consistent with the visual observations made in this study. Spectral analysis further confirmed that PyC particles of varying sizes originated from different plant materials. Notably, DRIFT spectra >2 mm revealed benzene carboxyl compounds, potentially derived from burnt plant materials such as lignin and pinoresinol, suggesting that these compounds may be derived from charred xylem [52].

The atomic ratio of PyC serves as a crucial indicator of its aromaticity, stability and polarity [53]. The International Biochar Association stipulates that an H/C atomic ratio < 0.7 signifies whether PyC has undergone sufficient thermochemical alteration [54]. Therefore, the four particle sizes of PyC examined in this study are entirely thermochemically transformed, exhibiting strong aromaticity and stability. Meanwhile, the van Krevelen plot indicates that the fractions within 1–2 mm and 0.5–1 mm were distributed in the charcoal zone, whereas the <0.5 mm fraction aligned near this zone. Hammes et al. [55] emphasized that the H/C atomic ratio in charcoal can effectively indicate the temperature to which plant material was subjected during a wildfire. Specifically, an H/C atomic ratio greater than 0.5 typically signifies char produced at temperatures below 500 °C, while char exhibiting an H/C ratio of less than 0.5 suggests that it was formed at elevated temperatures. Thus, it can be inferred that all the fractions in our study were produced under combustion conditions exceeding 500 °C.

Spokas et al. [56] developed a correlation between PyC stability and the O/C atomic ratio, suggesting that biochar with an O/C ratio below 0.2 has a half-life of over 1000 years. The half-life for ratios between 0.2 and 0.6 ranges from 100 to 1000 years, and for ratios > 0.6, it is less than 100 years. It is speculated that the four particle sizes of PyC in this study all have half-lives between 100 and 1000 years. When these PyC particles are leached into the

soil layer through precipitation, this stable time scale is likely to be further extended due to the protective effects of aggregates and minerals.

5. Conclusions

Thirteen years after the wildfire, this typical cold temperate coniferous forest fire accumulated 28.6 ± 17.0 Mg·ha^{-1} of PyC above-ground. WD residual PyC storage ranged from 0.040–0.179 Mg·ha^{-1}; PyC storage of the charcoal layer ranged from 7.9–44.3 Mg·ha^{-1}. The charcoal layer PyC storage is absolutely dominant, accounting for more than 99% of the total PyC in the upper part of the ground. This indicates that the PyC pool in this stage has essentially completed the flow from WD to the charcoal layer, and may even have occurred the flow and deposition of the soil layer. This allows us to clearly recognize the retention effects of the above-ground WD and charcoal layer, which are important components of the carbon sink in cold temperate coniferous forest.

Through atomic ratio analysis, it was confirmed that the charcoal layer PyC has a half-life ranging from 100 to 1000 years, indicating a low likelihood of chemical decomposition. It is highly probable that the charcoal layer PyC will be exported through slope migration, necessitating further research. Additionally, our study is influenced by the cumulative effects of historical fire disturbances. Therefore, future research should integrate tree fire scar records and BPCA molecular markers to construct a millennial-scale fire disturbance sequence and assess the statistical correlation between current PyC storage and historical fire disturbances.

Author Contributions: Y.P. and Y.Z. conceived the ideas and designed methodology; Y.P., L.S. and X.H. collected the data; Y.P. analysed the data; Y.P. and Y.Z. led the writing of the manuscript. All authors have read and agreed to the published version of the manuscript.

Funding: This work was financially supported by the National Natural Science Foundation of China (31570597) and Category D project of Central Colleges and Universities (HFW230600022).

Data Availability Statement: Data are contained within the article.

Conflicts of Interest: The authors have no conflicts of interest to declare.

References

1. Santín, C.; Doerr, S.H.; Preston, C.M.; González-Rodríguez, G. Pyrogenic organic matter production from wildfires: A missing sink in the global carbon cycle. *Glob. Change Biol.* **2015**, *21*, 1621–1633. [CrossRef] [PubMed]
2. Huang, W.T.; Hu, Y.M.; Chang, Y.; Liu, M.; Zhang, H.X.; Zhang, W. Advances on research of pyrogenic carbon in forests. *Chin. J. Ecol.* **2017**, *36*, 3257. [CrossRef]
3. Alexis, M.A.; Rasse, D.P.; Rumpel, C.; Bardoux, G.; Péchot, N.; Schmalzer, P.; Drake, B.; Mariotti, A. Fire impact on C and N losses and charcoal production in a scrub oak ecosystem. *Biogeochemistry* **2006**, *82*, 201–216. [CrossRef]
4. Hanke, U.M.; Eglinton, T.I.; Braun, A.L.L.; Reddy, C.M.; Wiedemeier, D.B.; Schmidt, M.W.I. Decoupled sedimentary records of combustion: Causes and implications. *Geophys. Res. Lett.* **2016**, *43*, 5098–5108. [CrossRef]
5. Czimczik, C.I.; Schmidt, M.W.I.; Schulze, E. Effects of increasing fire frequency on black carbon and organic matter in Podzols of Siberian Scots pine forests. *Eur. J. Soil Sci.* **2004**, *56*, 417–428. [CrossRef]
6. Reichstein, M.; Bahn, M.; Ciais, P.; Frank, D.; Mahecha, M.D.; Seneviratne, S.I.; Zscheischler, J.; Beer, C.; Buchmann, N.; Frank, D.C.; et al. Climate extremes and the carbon cycle. *Nature* **2013**, *500*, 287–295. [CrossRef]
7. Ottmar, R.D. Wildland fire emissions, carbon, and climate: Modeling fuel consumption. *For. Ecol. Manag.* **2014**, *317*, 41–50. [CrossRef]
8. Wang, J.; Xiong, Z.; Kuzyakov, Y. Biochar stability in soil: Meta-analysis of decomposition and priming effects. *Change Biol. Bioener.* **2016**, *8*, 512–523. [CrossRef]
9. Bird, M.I.; Wynn, J.G.; Saiz, G.; Wurster, C.M.; McBeath, A. The Pyrogenic Carbon Cycle. *Annu. Rev. Earth Planet. Sci.* **2015**, *43*, 273–298. [CrossRef]
10. Fang, Y.; Singh, B.P.; Krull, E. Biochar carbon stability in four contrasting soils. *Eur. J. Soil Sci.* **2014**, *65*, 60–71. [CrossRef]

11. Mašek, O.; Brownsort, P.; Cross, A.; Sohi, S. Influence of production conditions on the yield and environmental stability of biochar. *Fuel* **2013**, *103*, 151–155. [CrossRef]
12. Donato, D.C.; Campbell, J.L.; Fontaine, J.B.; Law, B.E. Quantifying Char in Postfire Woody Detritus Inventories. *Fire Ecol.* **2009**, *5*, 104–115. [CrossRef]
13. Chao, L.; Zhang, W.; Wang, S. Review on Biochar Decomposition and Priming Effect. *Earth Environ.* **2017**, *45*, 686–697. [CrossRef]
14. Biederman, L.A.; Harpole, W.S. Biochar and its effects on plant productivity and nutrient cycling: A meta-analysis. *GCB Bioenergy* **2013**, *5*, 202–214. [CrossRef]
15. Maestrini, B.; Nannipieri, P.; Abiven, S. A meta-analysis on pyrogenic organic matter induced priming effect. *GCB Bioenergy* **2015**, *7*, 577–590. [CrossRef]
16. Esteves, B.M.; Pereira, H.M. Wood modification by heat treatment: A review. *Bioresources* **2009**, *4*, 370–404. [CrossRef]
17. Preston, C.M.; Schmidt, M.W.I. Black (pyrogenic) carbon: A synthesis of current knowledge and uncertainties with special consideration of boreal regions. *Biogeosciences* **2006**, *3*, 397–420. [CrossRef]
18. Haukenes, V.L.; Asplund, J.; Åsgård, L.; Rolstad, J.; Storaunet, K.O.; Ohlson, M. Proportion of charcoal carbon in the forest floor carbon pool in relation to fire history in a boreal forest landscape. *Ecosphere* **2023**, *14*, e4713. [CrossRef]
19. Eckdahl, J.A.; Rodriguez, P.C.; Kristensen, J.A.; Metcalfe, D.B.; Ljung, K. Mineral Soils Are an Important Intermediate Storage Pool of Black Carbon in Fennoscandian Boreal Forests. *Glob. Biogeochem. Cycles* **2022**, *36*, e2022GB007489. [CrossRef]
20. Sayer, E.J. Using experimental manipulation to assess the roles of leaf litter in the functioning of forest ecosystems. *Biol. Rev.* **2006**, *81*, 1–31. [CrossRef]
21. Dymov, A.A. Soils of Post-Pyrogenic Forests. *Eurasian Soil Sci.* **2023**, *56*, S84–S113. [CrossRef]
22. Jenkins, M.E.; Bell, T.L.; Poon, L.F.; Aponte, C.; Adams, M.A. Production of pyrogenic carbon during planned fires in forests of East Gippsland, Victoria. *For. Ecol. Manag.* **2016**, *373*, 9–16. [CrossRef]
23. Cheng, Y.; Luo, P.; Yang, H.; Li, H.; Luo, C.; Jia, H.; Huang, Y. Fire effects on soil carbon cycling pools in forest ecosystems: A global meta-analysis. *Sci. Total. Environ.* **2023**, *895*, 165001. [CrossRef] [PubMed]
24. Mantel, S.; Dondeyne, S.; Deckers, S. World reference base for soil resources (WRB). *Encycl. Soils Environ.* **2023**, *4*, 206–217. [CrossRef]
25. Chen, H.; Hu, Y.; Chang, Y.; Bu, R.; Li, Y.; Liu, M.; Xiong, Z. Simulation of the effect of forest harvest mode on forest landscape: A case study in Huzhong forest region of Daxing' anling Mountains, China. *Chin. J. Ecol.* **2013**, *32*, 1888–1895. [CrossRef]
26. Guo, K.; Fang, J.-Y.; Wang, G.-H.; Tang, Z.-Y.; Xie, Z.-Q.; Shen, Z.-H.; Wang, R.-Q.; Qiang, S.; Liang, C.-Z.; DA, L.-J.; et al. A revised scheme of vegetation classification system of China. *Chin. J. Plant Ecol.* **2020**, *44*, 111–127. [CrossRef]
27. Yang, D.; He, H.-S.; Wu, Z.-W.; Liang, Y.; Huang, C.; Luo, X.; Xiao, J.-T.; Zhang, Q.-L. Influence of fire disturbance on aboveground deadwood debris carbon storage in Huzhong forest region of Great Xing'an Mountains, Northeast China. *Yingyong Shengtai Xuebao* **2015**, *26*, 331–339.
28. Yan, E.; Wang, X.; Huang, J. Concept and Classification of Coarse Woody Debris in Forest Ecosystems. *Front. Biol. China* **2005**, *1*, 76–84. [CrossRef]
29. Preston, C.M.; Simard, M.; Bergeron, Y.; Bernard, G.M.; Wasylishen, R.E. Charcoal in Organic Horizon and Surface Mineral Soil in a Boreal Forest Fire Chronosequence of Western Quebec: Stocks, Depth Distribution, Chemical Properties and a Synthesis of Related Studies. *Front. Earth Sci.* **2017**, *5*, 98. [CrossRef]
30. Nocentini, C.; Certini, G.; Knicker, H.; Francioso, O.; Rumpel, C. Nature and reactivity of charcoal produced and added to soil during wildfire are particle-size dependent. *Org. Geochem.* **2010**, *41*, 682–689. [CrossRef]
31. Rumpel, C.; Alexis, M.; Chabbi, A.; Chaplot, V.; Rasse, D.; Valentin, C.; Mariotti, A. Black carbon contribution to soil organic matter composition in tropical sloping land under slash and burn agriculture. *Geoderma* **2006**, *130*, 35–46. [CrossRef]
32. Ohlson, M.; Tryterud, E. Interpretation of the charcoal record in forest soils: Forest fires and their production and deposition of macroscopic charcoal. *Holocene* **2000**, *10*, 519–525. [CrossRef]
33. Rayment, G.E.; Lyons, D.J. *Soil Chemical Methods: Australasia*; CSIRO Publishing: Clayton, Australia, 2011; Volume 3.
34. Sun, J.; Sang, Y.; Song, J.; Cui, X. Content and distribution of black carbon in typical forest soils in Changbaishan Mountains. *J. For. Res.* **2016**, *29*, 34–40. [CrossRef]
35. Lim, B.; Cachier, H. Determination of black carbon by chemical oxidation and thermal treatment in recent marine and lake sediments and Cretaceous-Tertiary clays. *Chem. Geol.* **1996**, *131*, 143–154. [CrossRef]
36. Cai, H.; Di, X.; Jin, G. Carbon density of coarse woody debris in a spruce-fir valley forest in Xiaoxing'an Mountains, China. *Acta Ecol. Sin.* **2015**, *35*, 8194–8201. [CrossRef]
37. Wang, X.-L.; Chang, Y.; Chen, H.-W.; Hu, Y.-M.; Jiao, L.-L.; Feng, Y.-T.; Wu, W.; Wu, H.-F. Spatial pattern of forest biomass and its influencing factors in the Great Xing'an Mountains, Heilongjiang Province, China. *J. Appl. Ecol.* **2014**, *25*, 974–982. [CrossRef]
38. Waddell, K.L. Sampling coarse woody debris for multiple attributes in extensive resource inventories. *Ecol. Indic.* **2002**, *1*, 139–153. [CrossRef]
39. Guochun, L. Brief introduction to statistical software—SPSS. *J. Evid.-Based Med.* **2003**, *3*, 249–251,253. [CrossRef]

40. González-Pérez, J.A.; González-Vila, F.J.; Almendros, G.; Knicker, H. The effect of fire on soil organic matter—A review. *Environ. Int.* **2004**, *30*, 855–870. [CrossRef]
41. Fuente, E.; Menéndez, J.A.; Díez, M.A.; Suárez, D.; Montes-Morán, M.A. Infrared Spectroscopy of Carbon Materials: A Quantum Chemical Study of Model Compounds. *J. Phys. Chem. B* **2003**, *107*, 6350–6359. [CrossRef]
42. El-Hendawy, A.-N.A. Variation in the FTIR spectra of a biomass under impregnation, carbonization and oxidation conditions. *J. Anal. Appl. Pyrolysis* **2006**, *75*, 159–166. [CrossRef]
43. Knicker, H.; Hilscher, A.; González-Vila, F.J.; Almendros, G. A new conceptual model for the structural properties of char produced during vegetation fires. *Org. Geochem.* **2008**, *39*, 935–939. [CrossRef]
44. Tinker, D.B.; Knight, D.H. Coarse Woody Debris following Fire and Logging in Wyoming Lodgepole Pine Forests. *Ecosystems* **2000**, *3*, 472–483. [CrossRef]
45. Righi, C.A.; de Alencastro Graça, P.M.L.; Cerri, C.C.; Feigl, B.J.; Fearnside, P.M. Biomass burning in Brazil's Amazonian "arc of deforestation": Burning efficiency and charcoal formation in a fire after mechanized clearing at Feliz Natal, Mato Grosso. *For. Ecol. Manag.* **2009**, *258*, 2535–2546. [CrossRef]
46. Lehmann, J.; Solomon, D.; Kinyangi, J.; Dathe, L.; Wirick, S.; Jacobsen, C. Spatial complexity of soil organic matter forms at nanometre scales. *Nat. Geosci.* **2008**, *1*, 238–242. [CrossRef]
47. Kuzyakov, Y.; Subbotina, I.; Chen, H.; Bogomolova, I.; Xu, X. Black carbon decomposition and incorporation into soil microbial biomass estimated by ^{14}C labeling. *Soil Biol. Biochem.* **2009**, *41*, 210–219. [CrossRef]
48. Ahmad, M.; Rajapaksha, A.U.; Lim, J.E.; Zhang, M.; Bolan, N.; Mohan, D.; Vithanage, M.; Lee, S.S.; Ok, Y.S. Biochar as a sorbent for contaminant management in soil and water: A review. *Chemosphere* **2014**, *99*, 19–33. [CrossRef]
49. Major, J.; Lehmann, J.; Rondon, M.; Goodale, C. Fate of soil-applied black carbon: Downward migration, leaching and soil respiration. *Glob. Chang. Biol.* **2010**, *16*, 1366–1379. [CrossRef]
50. Brodowski, S.; Amelung, W.; Haumaier, L.; Abetz, C.; Zech, W. Morphological and chemical properties of black carbon in physical soil fractions as revealed by scanning electron microscopy and energy-dispersive X-ray spectroscopy. *Geoderma* **2005**, *128*, 116–129. [CrossRef]
51. Wang, M.; Cui, X.; Li, S.; Zhang, W.; Zhao, H. Effects of topographic factors on soil black carbon storage in coniferous forests at the north end of Greater Khingan Mountains. *J. Nanjing For. Univ. Nat. Sci. Ed.* **2021**, *45*, 151–158. [CrossRef]
52. Brodowski, S.; Rodionov, A.; Haumaier, L.; Glaser, B.; Amelung, W. Revised black carbon assessment using benzene polycarboxylic acids. *Org. Geochem.* **2005**, *36*, 1299–1310. [CrossRef]
53. Keiluweit, M.; Nico, P.S.; Johnson, M.G.; Kleber, M. Dynamic Molecular Structure of Plant Biomass-Derived Black Carbon (Biochar). *Environ. Sci. Technol.* **2010**, *44*, 1247–1253. [CrossRef] [PubMed]
54. Camps-Arbestain, M.; Amonette, J.E.; Singh, B.; Wang, T.; Schmidt, H.P. *A Biochar Classification System and Associated Test Methods, Biochar for Environmental Management*; Routledge: London, UK, 2015. [CrossRef]
55. Hammes, K.; Smernik, R.J.; Skjemstad, J.O.; Schmidt, M.W. Characterisation and evaluation of reference materials for black carbon analysis using elemental composition, colour, BET surface area and 13C NMR spectroscopy. *Appl. Geochem.* **2008**, *23*, 2113–2122. [CrossRef]
56. A Spokas, K. Review of the stability of biochar in soils: Predictability of O:C molar ratios. *Carbon Manag.* **2010**, *1*, 289–303. [CrossRef]